Surface landing of microtubule nanotracks influenced by lithographically patterned channels

Chih-Tin Lin,[1,a)] Ming-Tse Kao,[2] Edgar Meyhofer,[2,3,b)] and Katsuo Kurabayashi[1,3,b)]
[1]*Department of Electrical Engineering and Computer Science, University of Michigan, Ann Arbor, Michigan 48109, USA*
[2]*Department of Biomedical Engineering, University of Michigan, Ann Arbor, Michigan 48109, USA*
[3]*Department of Mechanical Engineering, University of Michigan, Ann Arbor, Michigan 48109, USA*

(Received 7 August 2009; accepted 18 August 2009; published online 8 September 2009)

Microtubules, which serve as cellular structural components in nature, can be placed within a lithographically patterned channel as engineered nanoscale tracks for bionanotechnology applications. We study the landing behavior of microtubules upon their diffusion onto a kinesin-coated glass surface in the presence of the channel. The influence of channel geometry on the landing rate of microtubules is experimentally characterized using channels with varying width. Additionally, we develop a theoretical model to quantitatively analyze our data by accounting for geometrical constraints due to both the width and height of the channels against the diffusion of the landing microtubules. © *2009 American Institute of Physics*. [doi:10.1063/1.3224194]

Nature has evolved highly efficient molecular machinery including kinesin biomotors that use cellular energy to move along microtubule cytoskeletal protein filaments of 25 nm in diameter and several micrometers in length. This motile mechanism is responsible for driving cellular activities, such as intercellular mass transport, cell division, and migration.[1,2] Recent research demonstrates significant potential of highly efficient kinesin-based molecular mass transport networks for bionanotechnology applications, including microscale device powering[3] and nanomaterial transport and assembly.[4,5] In such a molecular transport network, microtubule bundles with their structural polarity sorted along a lithographically patterned channel serve as user-directed nanoscale tracks for kinesin motors. The problem is, however, that the loading of microtubules onto a surface is inherently be impeded by geometrical constraints of the channel, thus potentially limiting the surface population of the constructed nanotracks. Only a limited number of studies[3] have been performed to characterize the surface landing behavior of microtubules affected by the presence of microfabricated channels.

In this letter, we quantitatively analyze the influence of a microfabricated channel on the diffusion of microtubules onto a kinesin-coated cover glass surface. We first construct channels of kinesin motility suppressing amorphous fluorocarbon polymer, CYTOP (Ref. 6) (Asahi Glass Co., Tokyo, Japan), on a cover glass chip by the standard photoresist lithography. Each sample chip has both a 200×200 μm^2 wide open area of blank glass and an array of open channels with their width of 3, 5, 10, and 20 μm. The fabricated open channels have a sidewall of 1.5 μm in height and 115 μm in length.

Prior to each of our assays, the entire chip surface is pretreated with aqueous solution of casein and then washed with BRB80 buffer. Bacterially expressed kinesin motors, NKHK560cys[7,8] are absorbed onto the exposed glass surface in the etched channel following a protein loading procedure identical to that for standard kinesin gliding assays. Chambers formed with a 100 μm thick glass spacer layer sandwiched between the aforementioned cover glass and another layer of glass substrate are loaded with kinesin (47 μg/ml casein and 1.6 μM kinesin in BRB80 buffer) and incubated for 5 min. Subsequently, microtubules in a BRB80 buffer containing 1 mM adenosine triphosphate (ATP) and an oxygen scavenger system (4 μg/ml microtubules, 2 mM MgCl2, 10 mM glucose, 100 μg/ml glucose oxidase, 80 μg/ml catalase, 10 mM dithiothreitol, and 47 μg/ml casein) are loaded. Here, we use tetramethyl rhodamine-labeled microtubules prepared using a protocol described in our previous study.[3] We observe samples with an inverted fluorescence microscope (Zeiss Axiovert 200, 40×, 1.3 NA Plan Neofluar objective), and take fluorescent images of the microtubules using a digital charge-coupled device camera (Orca II, Hamamatsu, Japan). To measure the microtubule landing rate, the number of microtubules landing onto the surface per unit time is counted from these images from 5 to 25 min after they are loaded (Fig. 1). We quantify the effect of channel width by the landing rate ratio, i.e., the ratio of the landing rate of microtubules diffusing onto the channel

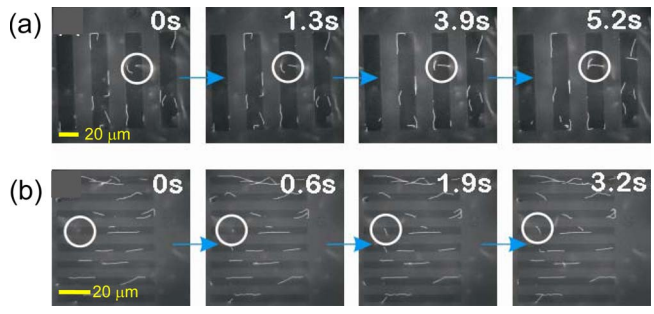

FIG. 1. (Color online) Image sequence of microtubule landing assays. A microtubule diffuses and lands onto the bottom surface of (a) 20 μm wide and (b) 5 μm wide microfabricated channels. The landing rate is obtained by averaging microtubule landing events per minute over all of the channels found in the entire field of view. These assays are performed in the presence of ATP molecules in solution.

[a)]Present address: Department of Electrical Engineering, National Taiwan University, Taipei 106, Taiwan.
[b)]Authors to whom correspondence should be addressed. Electronic addresses: meyhofer@umich.edu and katsuo@umich.edu.

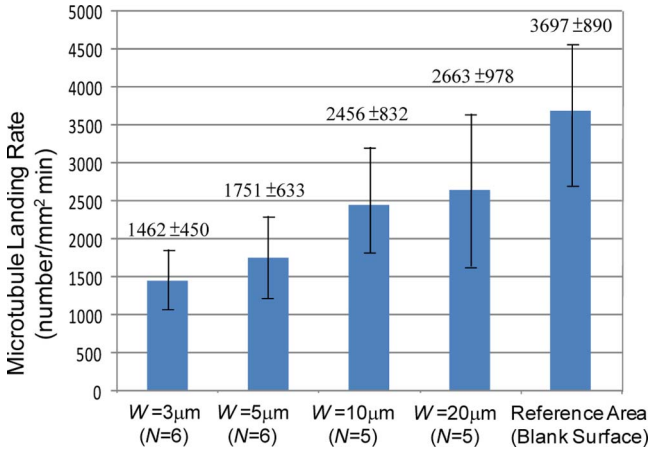

FIG. 2. (Color online) Microtubule landing rate obtained from assays with lithographically patterned channels with varying width. The standard deviation of each data is shown by the error bar.

bottom surface to that onto a wide open glass area (reference area) with no channel features. The landing rate varies proportional to kinesin motor density.[9,10] We expect nearly the same kinesin density for both the channel bottom and the open area as their surfaces are prepared in the same fashion on the common chip substrate. Figure 2 shows experimental results taken of various channel widths. All the landing rate data are normalized by the surface area to which the microtubules attach.

The average length of the microtubules in our study is 12 μm, which is more than two orders of magnitude shorter than its persistence length.[11–13] Thus, the microtubules can be modeled as straight cylindrical rods diffusing from solution into a microfluidic channel.[14] The channel sidewalls act as structural obstacles against microtubules diffusing from certain directions. Our model assumes that the microtubule diffusion occurs from all directions at the same probability and only onto the channel bottom surface of glass. The directions from which the microtubule can land onto the surface point without being blocked by the channel are determined by a few geometrical factors, including the channel width W, the channel sidewall height h, and the microtubule length L [Fig. 3(a)]. Since the channel is typically much longer than these parameters, we model it to be infinitely long for simplicity. The model neglects physical collisions between microtubules diffusing toward the surface. The relatively low microtubule

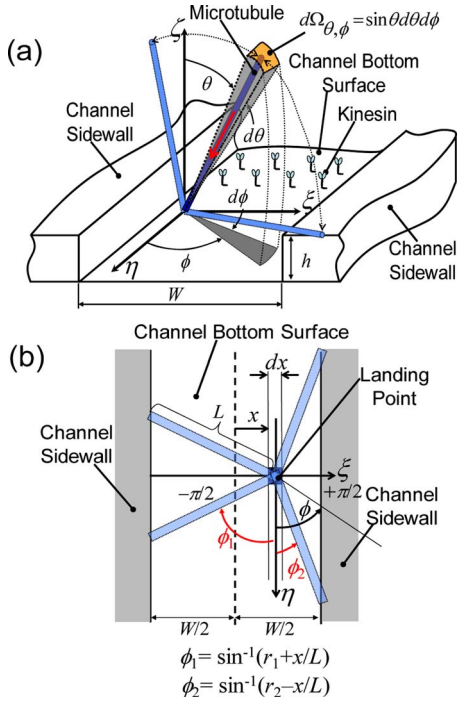

FIG. 3. (Color online) Schematic model for a microtubule landing event on the bottom surface of a microfabricated channel: (a) side view and (b) top view. The infinitesimal solid angle subtended by the polar angles of θ and $\theta+d\theta$ and the azimuthal angles of ϕ and $\phi+d\phi$ is given by $d\Omega_{\theta,\phi}=\sin\theta d\theta d\phi$. The local Cartesian coordinates denoted by the ξ-, η-, and ζ-axes are taken at the landing position between x and $x+dx$ across the channel. The ranges of the directional angles θ and ϕ associated with the diffusion directions of the microtubule are limited by the geometrical constraints that the channel sidewalls impose.

concentration used in our experiment is consistent with this assumption.

Now, we consider a microtubule reaching a landing point between x and $x+dx$ by diffusion [Fig. 3(b)]. The solid angle $\Omega(x)$ subtended by the angles of all the directions from which the microtubule is able to land onto the point is given by

$$\Omega(x) = 2\int_{-\pi/2}^{+\pi/2}\int_{0}^{f(\phi,x)} \sin\theta d\theta d\phi, \tag{1}$$

where the factor of 2 accounts for the geometrical symmetry with the azimuthal angle, $-\pi/2 \le \phi \le \pi/2$ and θ is the polar angle, $0 \le \theta \le f(\phi,x)$. The upper bound for its value $f(\phi,x)$ is determined by the geometrical constraints given by

$$f(\phi,x) = \begin{cases} \dfrac{\pi}{2} - \tan^{-1}\left[\dfrac{r_2\sin(-\phi)}{r_1+\dfrac{x}{L}}\right], & \dfrac{\pi}{2} \le \phi \le -\sin^{-1}\left(r_1+\dfrac{x}{L}\right) \\ \dfrac{\pi}{2}, & -\sin^{-1}\left(r_1+\dfrac{x}{L}\right) \le \phi \le \sin^{-1}\left(r_1-\dfrac{x}{L}\right) \\ \dfrac{\pi}{2} - \tan^{-1}\left[\dfrac{r_2\sin(\phi)}{r_1-\dfrac{x}{L}}\right], & \sin^{-1}\left(r_1-\dfrac{x}{L}\right) \le \phi \le -\dfrac{\pi}{2}, \end{cases} \tag{2}$$

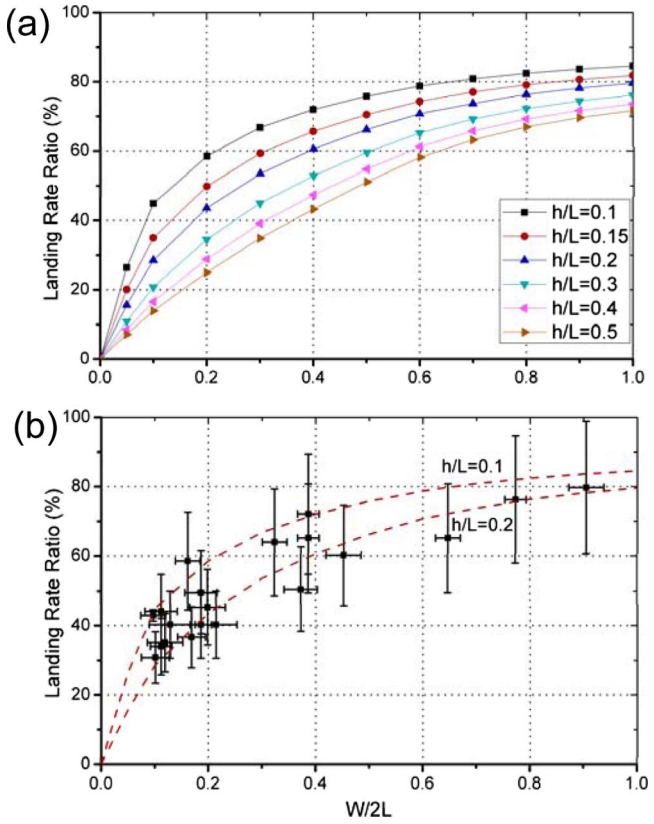

FIG. 4. (Color online) (a) Microtubule landing rate ratio as a function of the normalized channel width $W/2L$, which is calculated for various normalized sidewall heights. (b) Experimental results compared with model prediction. Each data point represents a ratio relative to the average value of the landing rate for the reference area. The vertical and horizontal error bars of each data point represent the standard deviation of the data sampling and the 95% confidence interval that results from the statistical distribution of the microtubule length for $N=100$, respectively.

where $r_1=W/2L$ and $r_2=h/L$, which are nondimensional channel shape factors.

The landing rate ratio R, which is the ratio of the landing rate of microtubules settling onto the channel bottom surface to that of microtubules diffusing toward the surface from all directions, is given by integrating $\Omega(x)/2\pi$ with respect to x across the entire channel as

$$R = \frac{1}{2\pi}\int_{-W/2}^{+W/2} \Omega(x)dx$$
$$= \frac{1}{\pi}\int_{-W/2}^{+W/2}\int_{-\pi/2}^{+\pi/2}\int_{0}^{f(\phi,x)} \sin\theta d\theta d\phi dx. \quad (3)$$

From Eq. (3), R is calculated with respect to the channel width at $0 \leq W \leq 2L$ for various channel heights [Fig. 4(a)]. The model indicates that the channel height needs to be $h < 0.2L$ to allow the microtubule landing event to occur at a probability higher than 80% for a channel width in this range. The value of R approaches 100% as W becomes sufficiently large ($W \gg L$) regardless of the channel height value. The landing rate of microtubules diffusing to the surface of channel bottom rapidly decreases with the channel width at $W < 0.5L$. A channel having narrow width ($W < 0.2L$) and large height ($h > 0.5L$) is predicted to yield poor settlement of microtubules with $R < 20\% - 50\%$ as a result of its severe geometrical constraints.

Figure 4(b) compares experimental results with our model prediction. Uncertainties in predicting experimental observations stem from two sources: (1) the actual microtubule length has a distribution ranging from 8 to 20 μm and (2) the average microtubule length varied slightly between 11 and 15 μm between different assays. These experimental uncertainties translate into a ratio of h/L of about 0.1–0.2 at a 95% confidence level with a sample of $N=2000$. Our model predicts the experimental results with its theoretical curves of this range of h/L well fitting to the data points within their standard deviations.

In summary, we have studied the effect of the presence of a microfluidic channel on the landing rate of microtubules diffusing onto a kinesin-coated glass surface, which results in preferential adsorption of short microtubules. This effect needs to be carefully considered to achieve a desired surface population of microtubule nanotracks upon their construction. Interestingly, the effect yields a phenomenon opposite to the one reported in a previous study using a thermally functional polymer surface.[15] Both the statistical model and the experimental results presented in this work provide quantitative guidelines on how one should design a microfluidic channel to retain a sufficient number of microtubules on a surface. For example, a channel design with width larger than 20 μm and height smaller than 1.5 μm is required to keep the reduction of the landing rate less than 20% for microtubules of ~10 μm in length. Our experimentally validated model may generally be applied to guide the design of engineered on-chip devices and structures that mimic the kinesin-based molecular transport network in a living cell using microtubule nanotracks.

This work was supported by DARPA Contract No. N66001-02-C. We thank the staff members of the University of Michigan Lurie Nanofabrication Facility for their support in our fabrication of microtubule guiding assay sample chips.

[1] J. Howard, Nature (London) **389**, 561 (1997).
[2] N. Hirokawa, Science **279**, 519 (1998).
[3] C. T. Lin, M. T. Kao, K. Kurabayashi, and E. Meyhofer, Small **2**, 281 (2006).
[4] R. K. Doot, H. Hess, and V. Vogel, Soft Matter **3**, 349 (2007).
[5] A. Goel and V. Vogel, Nat. Nanotechnol. **3**, 465 (2008).
[6] C. T. Lin, M. T. Kao, K. Kurabayashi, and E. Meyhofer, Nano Lett. **8**, 1041 (2008).
[7] A. Kallipolitou, D. Deluca, U. Majdic, S. Lakamper, R. Cross, E. Meyhofer, L. Moroder, M. Schliwa, and G. Woehlke, EMBO J. **20**, 6226 (2001).
[8] S. Lakamper, A. Kallipolitou, G. Woehlke, M. Schliwa, and E. Meyhofer, Biophys. J. **84**, 1833 (2003).
[9] W. O. Hancock and J. Howard, J. Cell Biol. **140**, 1395 (1998).
[10] A. I. Marcus, J. C. Ambrose, L. Blickley, W. O. Hancock, and R. J. Cyr, Cell Motil. Cytoskeleton **52**, 144 (2002).
[11] F. Gittes, B. Mickey, J. Nettleton, and J. Howard, J. Cell Biol. **120**, 923 (1993).
[12] J. C. Kurz and R. C. Williams, Biochemistry **34**, 13374 (1995).
[13] T. Kim, M. T. Kao, E. F. Hasselbrink, and E. Meyhofer, Biophys. J. **94**, 3880 (2008).
[14] C. Bouchiat, M. D. Wang, J. F. Allemand, T. Strick, S. M. Block, and V. Croquette, Biophys. J. **76**, 409 (1999).
[15] L. Ionov, M. Stamm, and S. Diez, Nano Lett. **6**, 1982 (2006).